

## Optical Mixing of Rydberg Angular Momenta

John D. Corless and C. R. Stroud, Jr.

*The Institute of Optics, University of Rochester, Rochester, New York 14627*

(Received 5 August 1996; revised manuscript received 3 March 1997)

When optical frequency fields are used to couple a ground state to a Rydberg state, the resonant dipole coupling is to a low angular momentum state. Higher angular momentum states are typically thought not to play a role in the excitation. The extremely large dipole matrix elements coupling Rydberg states of the same  $n$  but differing  $l$ , however, allow optical fields of modest strengths to produce Rabi frequencies larger than optical frequencies. We demonstrate that these optical fields can therefore readily excite the higher angular momentum states, and we examine the consequences of this coupling. [S0031-9007(97)03635-1]

PACS numbers: 42.50.Hz, 32.80.Bx, 32.80.Rm, 42.65.Ky

The degeneracy of the hydrogenic state with principal quantum number  $n$  is  $n^2$ . Thus, even modestly high Rydberg states with  $n = 50$  have thousands of higher angular momentum states. Generally laser excitation of these levels is achieved with one to three photons, each carrying one unit of angular momentum, so that only the lowest angular momentum states are assumed to be excited. Of course, various techniques using additional dc or low frequency electric and magnetic fields can be combined with the optical excitation to reach the high angular momentum states [1]. But, with simple optical field excitation, it is always assumed that the high angular momentum states can be safely ignored [2–4].

In this paper we will demonstrate that these high angular momentum states cannot be ignored, even with laser intensities as low as  $10^{10}$  W/cm<sup>2</sup>. The source of their importance is the enormous dipole moments coupling states with the same principal quantum number  $n$  but with orbital quantum number  $l$  differing by one. These dipole moments scale as  $n^2$  for  $l \ll n$  [5]. Of course, the detuning for transitions between these states induced by an optical field is the optical frequency. Significant transfer of population therefore requires that the Rabi frequency coupling these states exceed the optical frequency. This identifies a *critical intensity*,  $I_c$ , above which these degenerate states are strongly mixed. Surprisingly, for  $n = 30$  this critical field is only  $I_c \approx 10^{10}$  W/cm<sup>2</sup> and scales as  $n^{-4}$ .

Given that higher angular momentum states can be excited in these optical fields, the question then is whether other  $n$  manifolds also must be included. We consider a long pulse for which the Fourier bandwidth is small enough so that only one  $n$  manifold is resonantly coupled. To determine whether the dipole moment couplings are large, we make use of Heisenberg's correspondence principle [6]. For dipole moments between Rydberg states  $n$  and  $n'$  with  $\Delta n = n - n'$  the ratio of these dipole moments to the  $\Delta n = 0$  dipole moment is given for  $l \ll n$  by  $(2/3\Delta n)J'_{\Delta n}(\Delta n)$  with  $J'_{\Delta n}$  the derivative of the Bessel function of the first kind, order  $\Delta n$ . For  $\Delta n = 1$  this is  $\approx 0.2$  and for  $\Delta n = 2$  the ratio is  $\approx 0.07$ . The ratio continues to fall for increasing  $\Delta n$ . Thus, the smaller

dipole moments in conjunction with the long pulse enables us to formulate our model of the interaction ignoring neighboring  $n$  manifolds [7].

Figure 1 shows the level structure of our model. It consists of a ground state  $|g\rangle$  coupled by a laser field of frequency  $\omega_L$  to an  $nP$  Rydberg state,  $|l = 1\rangle$ . The Rydberg states are nearest-neighbor coupled to each other. Even though the optical photon energy is large enough to photoionize the Rydberg state, the associated cross sections are small and the dominant coupling at optical frequencies is to the degenerate states with opposite parity. With these approximations, the equations for the Rydberg state amplitudes,  $c_l$ , are

$$i\dot{c}_l = \omega_n c_l + f(t) \cos(\omega_L t) \left[ \delta_{l1} \Omega_g c_g + \sum_{l'=0}^{n-1} \Omega_{ll'} c_{l'} \right], \quad (1)$$

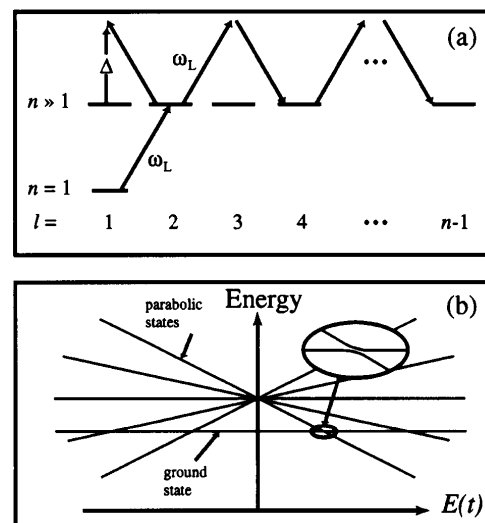


FIG. 1. Diagram of interaction. In (a) the ground state is coupled to the Rydberg  $P$  state. Each Rydberg state is coupled to its nearest neighbors with a detuning  $\Delta = \omega_L$ . In (b) the Stark map picture in the parabolic basis is shown where Rydberg energies are shifted linearly with optical electric field and have avoided crossings with the ground state.

where  $c_g$  is the ground state amplitude,  $\omega_n$  is the ground-to-Rydberg transition frequency,  $\delta_{ll}$  is the Kronecker delta indicating coupling to the  $P(l=1)$  state only, and  $\Omega_{ll'}$  is the Rydberg-to-Rydberg Rabi frequency. The applied optical field is taken to be linearly polarized in the  $z$  direction and given by  $E(t) = E_0 f(t) \cos(\omega_L t)$ , with  $f(t)$  the laser pulse envelope and  $E_0$  the amplitude. Because the Rabi frequencies,  $\Omega_{ll'}$ , are greater than  $\omega_L$  we cannot make the rotating-wave approximation [8]. We can, however, diagonalize the Rydberg-to-Rydberg coupling by transforming to the parabolic state basis,  $b_k = \sum_{l=0}^{n-1} S_{kl} c_l$ . These states are labeled by the electric quantum number  $k \in \{-n+1, -n+3, \dots, n-3, n-1\}$ .  $S_{kl}$  is the unitary transformation matrix whose components are proportional to Clebsch-Gordan coefficients [5]. The expense of this transformation is that every parabolic state is coupled to the ground state and has a time-dependent homogeneous term,

$$i\dot{b}_k = [\omega_n + \Delta_k f(t) \cos(\omega_L t)] b_k + S_{k1} \Omega_g f(t) \cos(\omega_L t) c_g. \quad (2)$$

The term  $\Delta_k = (3/2)nkE_0$  is the Stark shift of state  $k$  that a dc field of amplitude  $E_0$  would generate (within the single  $n$ -manifold approximation).  $S_{k1}$  represents the projection of the  $k$ th parabolic state onto the  $P$  state.

The ground-to-Rydberg-state Rabi frequency,  $\Omega_g$ , scales as  $n^{-3/2}$ . So for the intensity ranges considered this coupling can be treated perturbatively, giving  $c_g \approx 1$ . The approximate solution then is

$$b_k(t) = -i\Omega_g S_{k1} \exp\left[-i\omega_n t - i\frac{\Delta_k}{\omega_L} f(t) \sin(\omega_L t)\right] \times \int_{-\infty}^t dt' \frac{\omega_L}{\Delta_k} \exp(i\delta t') J_1\left[\frac{\Delta_k}{\omega_L} f(t')\right], \quad (3)$$

where  $\delta = \omega_n - \omega_L$  and  $J_1$  is the Bessel function of the first kind, order one. This solution assumes that  $\delta \ll \omega_L$  and that  $\omega_L \tau_p \gg 1$  where  $\tau_p$  is the pulse width. For hyperbolic secant pulses in the long-time limit, the solution can be expressed in terms of confluent hypergeometric functions. The spherical basis amplitudes are obtained by unitary transformation back to the original basis.

We now proceed to investigate the predictions of this model. To characterize the strength of the coupling we introduce the parameter  $\beta = (3/2)n(n-1)E_0/\omega_L$  which is the maximum value of the Stark shift,  $\Delta_k$ , measured in terms of the laser frequency  $\omega_L$ . Figure 2 shows the magnitude of the amplitudes in the spherical basis for  $\beta = 8$ . In Fig. 2(a) is shown the amplitudes at the peak of the laser pulse. The strong Rydberg-to-Rydberg coupling redistributes population among the higher angular momentum states. Because the Rabi frequency exceeds the optical frequency, the particular distribution of population changes considerably during an optical cycle. The figure empha-

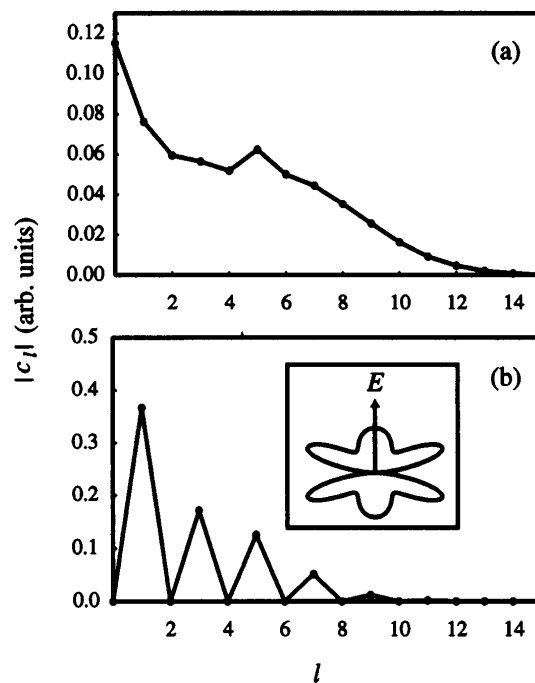


FIG. 2. Amplitudes of the Rydberg states in the spherical basis for  $\beta = 8$ . In (a), the amplitudes are at the peak of the pulse and in (b) at the end of the pulse. The resultant angular distribution is shown in the inset with the laser polarization direction indicated.

sizes the fact that a broad range of angular momentum states are transiently populated during the pulse and not only a given parity subset, which would be the case for  $\Delta l = 2$  Raman transitions [9]. For a smooth pulse profile, however, the states with parity opposite that of the  $P$  state have their population go smoothly back to zero so that at the end of the pulse, they are essentially unpopulated [see Fig. 2(b)]. The results are shown for the hyperbolic secant pulse, but are qualitatively the same for other smooth profiles.

Shown in the inset of the figure is the resultant angular distribution at the end of the pulse. The small  $\beta$  distribution is the familiar  $P$  state orbital with main probability lobes along the laser polarization axis. As the Rydberg-to-Rydberg coupling becomes larger than the optical frequency ( $\beta > 1$ ) the distribution becomes peaked orthogonal to the polarization direction. A signature of this effect was observed experimentally several years ago [10]. In that experiment, the angular distributions of photoionized electrons were measured as an intermediate resonance was tuned through the Rydberg series. For small  $n$  the distribution was peaked along the polarization direction. As  $n$  was increased the distribution, while still peaked along the polarization, began to bulge in the orthogonal direction. As  $n$  increases for a fixed field strength,  $\beta$  increases and we predict that the bound state distribution becomes elongated perpendicular to the polarization axis, but since photoionization cross sections decrease rapidly with

increasing  $l$ , mostly the small  $l$  component of the wave function will be photoionized. This leads to a photoion distribution which remains peaked along the polarization direction but begins to show increased probability in the orthogonal direction, as seen in Ref. [10]. A very similar distribution was observed in a high intensity experiment in xenon [11]. Evidence for this type of distribution was also seen in a theoretical study of the classical hydrogen atom in a strong electromagnetic field [12]. Similar angular distributions are seen for somewhat different reasons in molecules [13].

Another consequence of the excitation of these high angular momentum states can be seen by examination of Eq. (3). If we make a harmonic expansion of the first exponential in this equation we obtain

$$b_k(t) = r_k(t)e^{-i\omega_n t} \sum_{q=-\infty}^{\infty} J_q \left[ \frac{\Delta_k}{\omega_L} f(t) \right] e^{-iq\omega_L t}, \quad (4)$$

where  $r_k(t)$  is a slowly varying function. The Rydberg state amplitudes therefore oscillate at harmonics of the driving field depending on the ratio  $\Delta_k/\omega_L$ . The time-dependent dipole moment, given by the product of the ground state amplitude and these parabolic state amplitudes, will therefore also oscillate at harmonics of the driving field. Figure 3 shows the Fourier transform of the dipole moment. Only odd harmonics are generated, and furthermore they display the typical high harmonic spectrum of a rapid falloff followed by a relatively flat plateau region followed by a rapid cutoff [14]. It is interesting to note that for  $n = 65$  this power spectrum is predicted to occur for  $I \approx 6 \times 10^{11}$  W/cm<sup>2</sup>.

High harmonic generation has been predicted from several models [15]. This interaction, however, makes possible high harmonic generation at relatively low intensity. It also provides the possibility for enhancing the conversion efficiency. Since the dipole moment is proportional to the product of the ground and Rydberg state amplitudes, if the atom is prepared initially with some population in the Rydberg states, then the dipole moment will be increased. Thus by varying the initial population in the Rydberg state, the conversion efficiency can be adjusted.

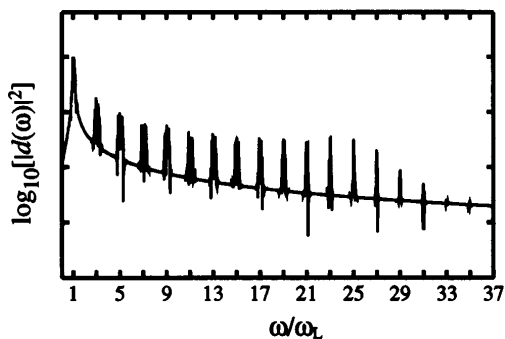


FIG. 3. Fourier transform of time-dependent dipole moment for  $\beta = 32$ .

Because the Rydberg-Rydberg Rabi frequencies are the largest parameters in our problem the physics is better understood via a simple model in which we treat the optical field as though it produces a dc Stark shift of the Rydberg states which is modulated at the optical frequency. Figure 1(b) shows the Stark map picture of our model. Each parabolic state has its energy [the homogeneous term in Eq. (2)] modulated at the optical frequency. This energy varies from  $\omega_n - \Delta_k$  to  $\omega_n + \Delta_k$  in one-half optical cycle as the electric field varies from  $-E_0$  to  $E_0$ . The ground state is unshifted. For simplicity, we take the pulse to be square for this analysis. Each state that has  $|\Delta_k| > \omega_n$  will have two avoided crossings with the ground state per optical cycle. Between the crossings, the free evolution of each state leads to a phase accumulation that can cause the two transition amplitudes to interfere. This interference is the analog of Stückelberg oscillations in inelastic atomic collisions [16] and has been recently observed in microwave multiphoton transitions [17].

Landau-Zener (LZ) theory can be used to describe how population changes during these anticrossings [18]. The transition probability in LZ theory is determined by the parameter

$$\Gamma = \frac{|\langle 1|V|2 \rangle|^2}{d\omega/dt}, \quad (5)$$

where  $V$  is the interaction term coupling state  $|1\rangle$  to  $|2\rangle$  and  $\omega$  is the energy difference between the two states [19]. The probability of an adiabatic transition is  $P_A = 1 - e^{-2\pi\Gamma}$ . In our case,  $V \propto \Omega_g$  and  $d\omega/dt \propto \omega_L \Delta_k$  so  $P_A \approx 2\pi\Gamma \ll 1$  and the transition is diabatic. So the population begins in the ground state, makes two diabatic crossings, and returns to the ground state with essentially no population transferred in one optical cycle. However, there are *many* cycles in our optical pulse. So, for the right phase accumulation between the crossings, many small transition amplitudes can add coherently to produce significant population transfer to the parabolic state.

To lowest order in  $P_A$ , the  $N$ -cycle transition probability is

$$P_{k \leftarrow g} = 8\pi N^2 \Gamma_k^2 \sin^2(\alpha_k - \phi_k) \frac{\sin^2(\delta\tau_p/2)}{(\delta\tau_p/2)^2}, \quad (6)$$

where  $\delta = \omega_n - \omega_L$ . The dynamical phase, analogous to the Stückelberg phase, is

$$\alpha_k = \omega_n t_k + (\Delta_k/\omega_L) \sin(\omega_L t_k), \quad (7)$$

and  $\phi_k$  is the phase associated with the LZ transition [20]. The time when state  $k$  crosses the ground state in the first cycle is given simply by

$$t_k = (1/\omega_L) \cos^{-1}(-\omega_n/\Delta_k). \quad (8)$$

The single crossing transfer probability is  $2\pi\Gamma_k$  with

$$\Gamma_k = \frac{S_{k1}^2 \Omega_g^2 \cos^2(\omega_L t_k)}{|\Delta_k \omega_L \sin(\omega_L t_k)|}. \quad (9)$$

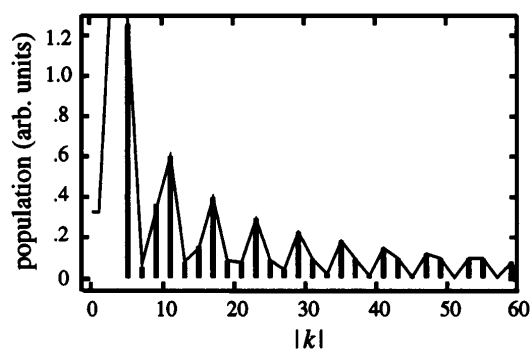


FIG. 4. Comparison of Eq. (3) (solid line) to Landau-Zener theory (vertical bars) for population in parabolic states with  $\beta = 30$ ,  $n = 60$ , and  $\delta = 0$ .

The presence of the traditional perturbation theory absorption profile shows the importance of matching the driving frequency  $\omega_L$  to the resonance frequency  $\omega_n$ . When the detuning is greater than the inverse pulse width, contributions from successive optical cycles interfere destructively. Therefore neighboring  $n$  states do not get populated even though they have shifts large enough to have avoided crossings with the ground state.

Figure 4 compares the predictions of the LZ theory to those of Eq. (3) for a square pulse. This simple LZ model assumes that each state has an avoided crossing with the ground state. This is in general not true for states near  $k = 0$  because they can have  $|\Delta_k| < \omega_n$ . Because of this, states near  $k = 0$  are not shown in the plot. In order that most states cross the ground state for this calculation we chose  $\beta = 30$ . Within these limits of applicability of this rather simple model the agreement is quite striking. In general, even for smaller  $\beta$  this model works well for those states that have  $|\Delta_k| > \omega_n$ . The agreement between the LZ theory and Eq. (3) is independent of the number of optical cycles for  $N \gg 1$ .

In conclusion, we have shown that the large Rydberg-to-Rydberg dipole moments lead to strong mixing of angular momentum states by optical frequency fields of relatively moderate intensities. Rabi frequencies exceeding optical frequencies give rise to significant redistribution of population to higher angular momentum states. Furthermore, the use of Landau-Zener level crossing theory can be used to understand some of the unique behaviors of these strongly driven Rydberg states.

The authors are grateful to I.Sh. Averbukh and J.H. Eberly for stimulating discussions. This work was par-

tially supported by the Army Research Office, the United States-Israel Binational Science Foundation, and the Department of Education.

- 
- [1] R. G. Hulet and D. Kleppner, Phys. Rev. Lett. **51**, 1430 (1983).
  - [2] J. A. Yeazell, M. Mallalieu, and C. R. Stroud, Jr., Phys. Rev. Lett. **64**, 2007 (1990).
  - [3] M. V. Fedorov and A. M. Movsesian, J. Opt. Soc. Am. B **6**, 928 (1989).
  - [4] H. Gratl, G. Alber, and P. Zoller, J. Phys. B **22**, L547 (1989).
  - [5] T. F. Gallagher, *Rydberg Atoms* (Cambridge University Press, Cambridge, 1994).
  - [6] J. Picart, A. R. Edmonds, and N. T. Minh, J. Phys. B **11**, L651 (1978).
  - [7] The ac Stark, or ponderomotive, shift of these levels is small and can be shown to be  $(1/n)$  times the spacing between Rydberg levels for  $I \approx I_c$ .
  - [8] B. Piraux and P. L. Knight, Phys. Rev. A **40**, 712 (1989).
  - [9] Redistribution to high angular momentum states via Raman coupling was considered in R. Grobe, G. Leuchs, and K. Rzazewski, Phys. Rev. A **34**, 1188 (1986); G. K. Ivanov, G. V. Golubkov, and D. M. Manakov, Zh. Eksp. Theor. Fiz. **106**, 1306 (1994).
  - [10] G. Leuchs and S. J. Smith, J. Sov. Laser Res. **6**, 296 (1985).
  - [11] B. Yang *et al.*, Phys. Rev. Lett. **71**, 3770 (1993).
  - [12] G. A. Kyrala, J. Opt. Soc. Am. B **4**, 731 (1987).
  - [13] B. Friedrich and D. Herschbach, Phys. Rev. Lett. **74**, 4623 (1995).
  - [14] See the article by A. L'Huillier, L.-A. Lompré, G. Mainfray, and C. Manus, in *Atoms in Intense Laser Fields*, edited by M. Gavrilu (Academic Press, San Diego, 1992).
  - [15] R. Burlon *et al.*, J. Opt. Soc. Am. B **13**, 162 (1996); B. Sundaram and P. W. Milonni, Phys. Rev. A **41**, 6571 (1990).
  - [16] E. C. G. Stückelberg, Helv. Phys. Acta **5**, 369 (1932).
  - [17] M. Gatzke, R. B. Watkins, and T. F. Gallagher, Phys. Rev. A **51**, 4835 (1995).
  - [18] Landau-Zener theory was applied in the case of Floquet level crossings due to large ground state Stark shifts in J. G. Story, D. I. Duncan, and T. F. Gallagher, Phys. Rev. Lett. **70**, 3012 (1993); J. G. Story, D. I. Duncan, and T. F. Gallagher, Phys. Rev. A **50**, 1607 (1994).
  - [19] J. R. Rubbmark, M. M. Kash, M. G. Littman, and D. Kleppner, Phys. Rev. A **23**, 3107 (1981).
  - [20] B. M. Garraway and S. Stenholm, Phys. Rev. A **46**, 1413 (1992).